Available online at www.sciencedirect.com
ScienceDirect
Journal of Crystal Growth 300 (2007) 50–56
JOURNAL OF CRYSTAL GROWTH
www.elsevier.com/locate/jcrysgro

Effect of island coalescence on structural and electrical properties of InN thin films

V. Lebedev[a,*], V. Cimalla[a], F.M. Morales[b], J.G. Lozano[b], D. González[b], Ch. Mauder[a], O. Ambacher[a]

[a]*Institute of Micro- and Nanotechnolgies, Technical University Ilmenau, D-98684 Ilmenau, Germany*
[b]*Dpto de Ciencia de los Materiales e Ingeniería Metalúrgica y Química Inorgánica, Facultad de Ciencias, Universidad de Cádiz, 11510 Puerto Real-Cádiz, Spain*

Abstract

In this work, coalescence aspects of InN epitaxy are addressed. The coalescence phenomena have been studied in thin InN epilayers by means of electron microscopy and X-ray diffraction. Coalescence time and the corresponding diffusion coefficients at elevated temperatures were estimated for InN deposition. The substrate temperature was found to impact drastically the coalescence of the epilayer, and consequently, the electrical and transport properties of hexagonal InN material. Additionally, a simple growth model was suggested to explain the formation of domain boundaries and (0 0 0 1) stacking faults formed during the coalescence. In particular, it is shown that two adjacent and tilted, hexagonal-shaped InN domains may form a non-coherent boundary along a $\{1\,\bar{1}\,0\,0\}$ plane. We also suggest that the interaction between tilted domains induces formation of basal dislocations. This interaction has two consequences: a localized lateral growth of the most epitaxially oriented domain (forming a basal (0 0 0 1) stacking fault) followed by the formation of a surface step, and consequently the termination of a threading dislocation by its dissociation and propagation under the formed (0 0 0 1) stacking fault.

PACS: 81.05.Ea; 81.15.Hi; 68.55.Ac; 68.55.Ln; 68.55.Jk; 68.55.Nq; 61.72.Lk; 61.72.Hh

Keywords: A1. Coalescence; A3. Molecular beam epitaxy; B1. InN

1. Introduction

The superior electronic properties make InN a highly potential material for the fabrication of high-frequency heterojunction field effect transistors [1]. Another important discovery about 2H-InN is its very strong surface charge accumulation on the order of $10^{13}\,cm^{-2}$ [2] revealing the promising applications of InN epilayers as chemical and biological sensors [3]. Recently reported results show also that THz emission from InN layers under excitation of ultrafast optical pulses exceeds those observed from p-InAs [4].

Recently, great progress in fabricating high-quality InN epilayers has been achieved [5]. Extensive research of material and device properties has been accomplished by a number of studies concerning defects, impurities and associated growth mechanisms [6–10]. However, a lack of lattice-matched substrate remains a main challenge hindering the progress on the practical side. Moreover, there are still substantial problems concerning a deep understanding of the fundamental mechanisms of the InN heteroepitaxy.

Epitaxial 2H-InN layers, which can be used for device fabrication are usually highly faulted single crystals and typically adopt a mosaic structure with subgrain boundaries delineated by threading dislocations (TDs) [9–12]. The origin of this structure is related to surface atomic processes during growth. In order to improve growths in a systematic way it is essential to understand the underlying kinetic processes such as adsorption, desorption, and surface diffusion. In particular, adatom diffusion on the growing surfaces is considered to be a key parameter

*Corresponding author. Tel.: +49 3677 693410; fax: +49 3677 693355.
E-mail address: vadim.lebedev@tu-ilmenau.de (V. Lebedev).

0022-0248/$ - see front matter © 2007 Published by Elsevier B.V.
doi:10.1016/j.jcrysgro.2007.02.003

controlling the coalescence and consequently the material quality and the surface morphology [13].

It was recently shown [14] that heteroepitaxy of InN on highly mismatched substrates can be divided into four stages, each of them having a critical impact on the crystal quality of the epilayer. In the framework of the suggested growth model the following stages of the strain relief have been proposed: plastic relaxation of strain by the introduction of geometric misfit dislocations, elastic strain relief during the island growth, formation of TDs induced by the coalescence of the islands, and relaxation of the elastic strain by introduction of secondary misfit dislocations. Additionally, edge type TDs and dislocations of mixed character have been found to be dominating defects in 2H-InN layers. It was demonstrated that TDs are active suppliers of the electrons and an exponential decay of their density with the thickness implies the corresponding decay in the carrier density. Room temperature mobilities in excess of $1500\,cm^2\,V^{-1}\,s^{-1}$ were obtained for ~800 nm thick InN layers with the dislocation densities of $\sim 3\times10^9\,cm^{-2}$ [14]. The proposed model emphasizes the determining role of the coalescence process in the formation of a dislocation network in heteroepitaxially grown 2H-InN.

Nucleation and subsequent coalescence are interesting and important problems, which control a number of physical and mechanical properties of thin films [15,16]. However, most of the studies were devoted to computer simulations of the grain growth in the isotropic limit (i.e., when both energy and mobility of grain boundaries are isotropic), with rare attempts on anisotropy calculations [17]. In the case of the heteroepitaxy of thin 2H-InN films, both energy and mobility are strongly anisotropic, e.g., their values depend on the misorientation between two neighbouring crystals and the spatial orientation of their boundaries. In addition, non-equilibrium growth conditions and the presence of liquid phase at the grain boundaries, usual for a group-III-rich growth, may also result in a strong anisotropy of both energy and mobility. Due to their complexity, either analytical or computational studies of the coalescence in 2H-InN have been never addressed.

Recently, we have proposed elsewhere [14,26] that the coalescence process is a dominating factor controlling key crystal properties as polytypism, dislocation density and surface morphology of 2H-InN. However, the island coalescence process was not discussed in detail. The present work is primarily focused on coalescence of 2H-InN islands and its impact on epilayer properties. Coalescence times and the corresponding diffusion coefficients at elevated temperatures were estimated (in the case of a 10-nm-thick InN epilayer). Additionally, a simple growth model is proposed to explain the formation of domain boundaries and stacking faults during the coalescence stage.

2. Experimental procedure

The samples were grown in a Balzer's plasma-induced molecular beam epitaxy (PIMBE) system described elsewhere [14]. The substrate temperatures were calibrated by an infra-red pyrometer. The growth process was monitored by digitized patterns of RHEED. Molecular fluxes were monitored *in situ* by a quadrupole mass-spectrometer and calibrated using RHEED oscillations. The samples consisted of epitaxial (0 0 0 1) AlN/Al_2O_3 and GaN/Al_2O_3 templates overgrown *in situ* by a 2H-InN epilayer at T_{sub}~380 °C. In these conditions, the growth rate is proportional to the impinging group-III flux thus getting sticking coefficients approximately equal to unity [18]. The InN epilayers were grown under stoichiometric (1:1) conditions to prevent surface metal accumulation. The thickness of the InN layer has been varied from 0.35 to 2.2 μm. More details on template preparation procedure and growth conditions can be found elsewhere [14,19].

Structural analysis was performed by high-resolution X-ray diffraction (XRD) using a Bruker D8 diffractometer. Rocking curves at the symmetric (0 0 0 2) and reciprocal space maps at the symmetric (0 0 0 2) and the asymmetric (20–25) InN reflections were taken to evaluate the crystal quality and the residual strain, respectively. The lowest FWHM of 0.270° was found at ~1 μm indicating the continuous improvement of the InN layers up to this thickness and a change in the relaxation mechanism thereafter. Thick InN layers of ~1 μm have only a small residual stress <0.1%. Transmission electron microscopy (TEM) was performed in electron microscopes operating at 200 keV (TECNAI 20S-TWIN (FEI) and JEM-2011 from JEOL). Mechanical thinning and ion milling were used to prepare specimens for cross-section inspection. Electron diffraction patterns and micrographs obtained in bright-field (BF) and dark-field (DF) modes by conventional two-beam (2B) conditions and high-resolution TEM (HRTEM) were obtained and analysed.

3. Results and discussion

The growth mode of an epilayer is determined by both bulk thermodynamics and surface kinetics. However, at non-equilibrium conditions characteristic for InN PIMBE, surface kinetics plays often a dominant role, especially during the early stages of nucleation and growth. In general the shape and size of nucleated 2H-InN nano-crystals depends on the crystal structure, temperature and composition (e.g. stoichiometry) [20]. In many cases, these islands have a hexagonal form with small degrees of truncation (see Fig. 1). This shape occurs since it leads to surface energy minimization for nuclei formed at equilibrium, and because of kinetics where the shape is determined by the rate at which different crystal faces grow [21]. However, the combination of factors such as temperature, kinetics, impurities, and surface energy effects could lead to unusual nanoparticle size-shape distributions, which influences the particle coalescence.

Fig. 1(d) shows an initial stage of nucleation and coalescence of 2H-InN domains during the deposition on GaN (0 0 0 1). An estimation of the coalescence time (τ_c) for

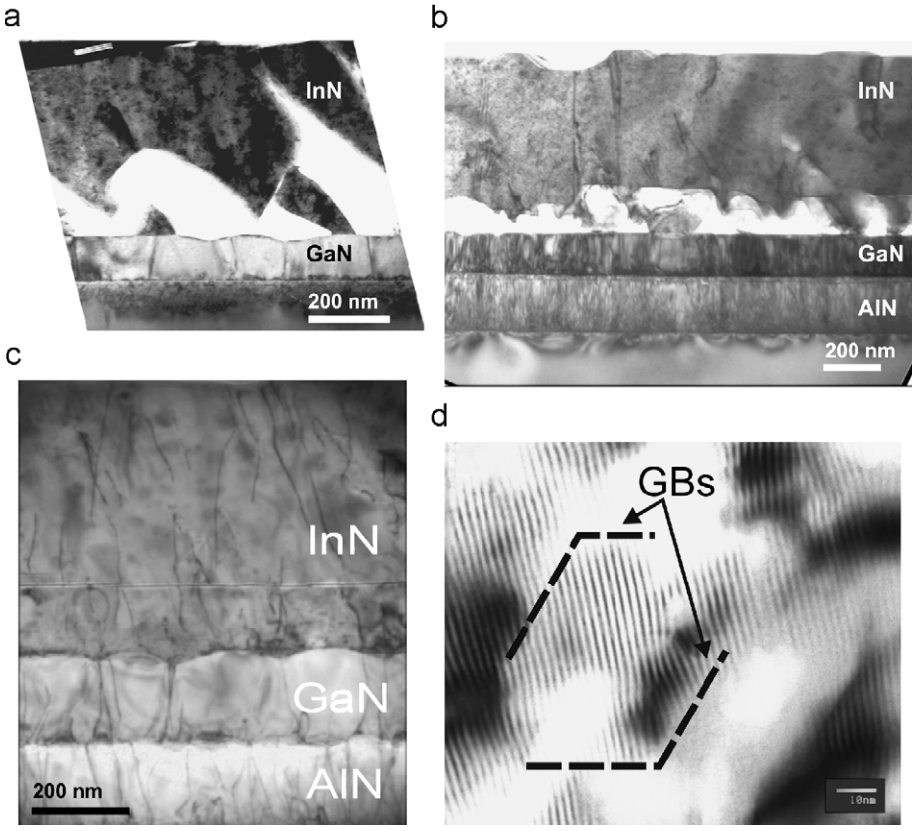

Fig. 1. Impact of completion of the coalescence on the TD density in 2H-InN epilayers illustrated by bright field TEM images. (a) Columnar structure of the epilayer grown at 500 °C weakly supported by the substrate (the columns are free of TDs). (b) The epilayers after partial coalescence at 450 °C (a few TDs appeared). (c) Continuous epilayer grown at 370 °C; coalescence is completed resulting in appearing dense TD network. (d) Plan-view TEM of the mosaic structure of a 10 nm thick InN layer.

islands of average diameter of ~60 nm yields a value of about 35 s. The driving forces for the high rate of lateral growth and consequently, of the coalescence is the surface diffusion of adsorbed species. Adatoms diffuse on the island surface from the regions of high curvature (fewer neighbours and therefore less strongly bound) towards the regions of lower curvature (e.g. facets) providing lateral growth of the initial nuclei [21]. Macroscopic theories of coalescence via atomic surface diffusion predict a coalescence time [22]:

$$\tau_c = \frac{kT}{CD_s(T)\gamma}\left(\frac{R}{a}\right)^4, \quad (1)$$

where R~30 nm is the domain radius, γ is the surface energy of InN(0 0 0 1), $C \approx 25$ is a numerical constant, $D_s(T)$ is the surface diffusion coefficient, $T = 370$ °C is the growth temperature, and a~0.3 nm is the inter atomic dimension.

For the case shown in Fig. 1(d) we obtain very low $D_s(370\,^\circ\mathrm{C}) \sim 6 \times 10^{-16}\,\mathrm{m^2\,s^{-1}}$ using the experimental value of $\tau_c = 35$ s. Thus, the estimated distance that an atom travels within the coalescence time τ_c using the relation $\lambda_{dif} = (D_s\tau_c)^{1/2}$ is λ_{dif}~0.14 μm which is only slightly larger than the crystal size after the coalescence. On the other side, observed flat-top InN pyramids indicate a significant lateral growth rate. Such a shape favours a rapid coalescence and a flatter morphology of the thicker films [21]. The presented estimations, however, assume a serious simplification of the real processes. The presence of various structural features (i.e. steps, kinks, and facets) [20,23] and Ostwald ripening [21,24] has to be taken into account.

As a consequence of the hexagonal symmetry of the initial 2H-nuclei, two kinds of domain boundaries can be formed during the coalescence lying on $\{1\,1\,\bar{2}\,0\}$ and $\{1\,0\,\bar{1}\,0\}$ planes. Such domain boundaries have been studied experimentally by Xin et al. [12] using $\mathbf{g}\cdot\mathbf{R}$ and HRTEM analyses and theoretically by Northrup et al. [25] for the case of 2H-GaN epilayers. A general model suggests a single growth fault on the basal plane of one island exhibiting a displacement relative to an unfaulted island. Thus, both $\{1\,\bar{2}\,1\,0\}$ and $\{1\,\bar{1}\,0\,0\}$ boundaries were considered to be of the stacking mismatch boundary (SMB) type. It was suggested that the $\{1\,\bar{2}\,1\,0\}$ boundary, having a displacement of magnitude and direction $\frac{1}{2}\langle 1\,0\,\bar{1}\,1\rangle$, arises from the coalescence of two islands, one of which is associated with a single growth fault on the basal plane. The $\{1\,\bar{1}\,0\,0\}$ boundary has been proposed to originate at

the epilayer/substrate interface and runs through the whole epilayer with a displacement of $1/3n\langle 1\,1\,\bar{2}\,0\rangle$ ($n>3$) in the basal plane and with an additional shift along $\langle 0\,0\,0\,1\rangle$, although the exact magnitude of the displacement of this boundary was not determined [12]. Because basal plane stacking faults are of low energy, they were proposed as the origin of SMBs.

Additionally, the formation of the grain boundaries on both planes was studied recently for the case of 2H-GaN selective epitaxy using 60 nm wide $\langle 1\,1\,\bar{2}\,0\rangle$ and $\langle 1\,0\,\bar{1}\,0\rangle$ grooves in Si_xN_y/Al_2O_3 templates [26]. It was observed that the grain boundaries are predominantly formed along $\langle 1\,\bar{1}\,0\,0\rangle$ planes. The domain interaction on $\langle 1\,1\,\bar{2}\,0\rangle$ plane family is rather poor leading to the degeneration of the $\langle 1\,1\,\bar{2}\,0\rangle$ contact interfaces to the grain boundaries along $\langle 1\,\bar{1}\,0\,0\rangle$ planes. This can be explained by the fact that boundaries along $\langle 1\,\bar{1}\,0\,0\rangle$ planes have the lowest energies as well as the lowest mobilities [27,28]. Therefore, energy minimization would make nuclei tend to bond by low-energy boundaries [17].

In Fig. 2(b), a TEM image shows domain boundaries lying on $\langle 1\,\bar{1}\,0\,0\rangle$ planes in an InN/GaN epilayers grown on AlN/sapphire template. The SMB network of the underlying GaN layer propagates into the topmost 2H-InN being responsible for the primary domain structure. On the other hand, a large InN/GaN mismatch results in the secondary domain structure with a characteristic domain size of ~50–60 nm [14]. The probable vertical displacement of the neighbouring domains leads to the (0 0 0 1) atomic plane disregistries. Such disregistries are highlighted in Fig. 2(a), where the HRTEM micrograph shows the shift between (0 0 0 1) basal planes approaching both sides of the SMB planes in 2H-InN epilayers.

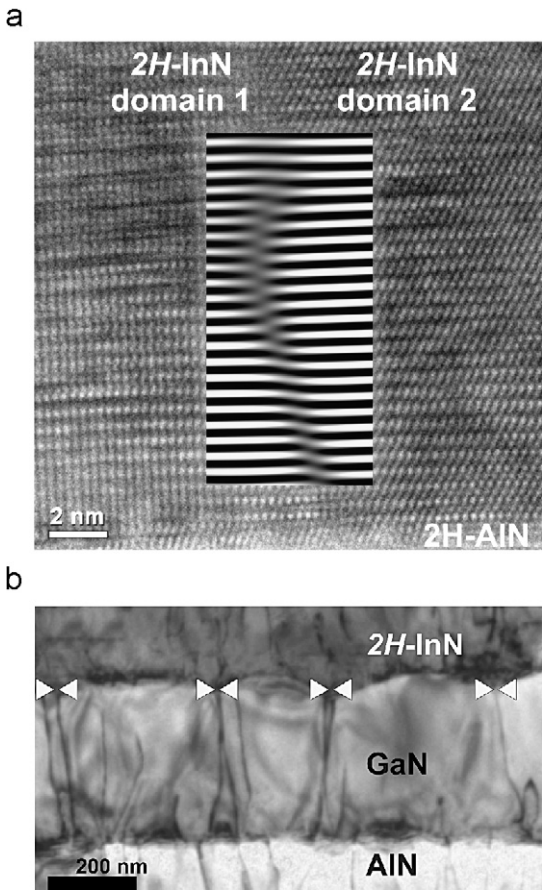

Fig. 2. (a) HRTEM image of a 2D DB between two 2H-InN domains placed on AlN template. (b) TEM of a 2D SMB network in a 2H-GaN epilayer after the partial coalescence of domains (triangles point out 2D boundaries).

A simple growth model, which is different to the one suggested by Xin et al. can be proposed to explain the formation and annihilation of the SMBs formed during the coalescence. The nucleation of highly mismatched 2H-InN material leads to the growth of islands having a slight deviation in the *c*-axis orientation (see Fig. 2(a)). Earlier, we have demonstrated that tilt (rotation along an axe parallel to the basal plane) and twist (rotation along an axe normal to the basal plane) of the simultaneously growing domains with respect to each other and to the *c*-axis of the substrate is characteristic for highly mismatched systems with a mismatch $f>10\%$; e.g. 2H-AlN/Si [29,30] and 2H-InN/AlN [14]. The magnitude of the tilt depends on the magnitude of the epilayer/substrate mismatch and on the actual growth conditions. It was also suggested that the origin of the tilt on the (0 0 0 1) basal plane is a partial accommodation of the residual mismatch in certain crystallographic directions.

In Fig. 2(a), a HRTEM micrograph of two slightly tilted 2H-InN domains is presented. They form a low-angle (~0.9° between $\langle 0\,0\,0\,1\rangle$ directions) SMB along $\langle 1\,\bar{1}\,0\,0\rangle$ planes. Similarly to the work by Xin et al., the magnitude of the local displacement vector along $\langle 0\,0\,0\,1\rangle$ does not exceed $\frac{1}{2}\langle 0\,0\,0\,1\rangle$. The maximum vertical displacement between the topmost (0 0 0 1) planes of two domains in contact, *b*, can be calculated using a tilt angle α and a domain radius $d\sim 100$ nm as $b\sim d\tan\alpha = 1.57$ nm. A high magnitude of the total displacement has two important consequences for the coalescence: Firstly, tilted domains form a non-coherent boundary along the $\langle 1\,\bar{1}\,0\,0\rangle$ plane. Additionally, the local displacement of the (0 0 0 1) planes is not constant, but does not exceed $c/2$. Secondly, as it is schematically shown in Fig. 3(a), the interaction of a tilted terminating (0 0 0 1) plane with the wall of a neighbouring well-oriented (heteroepitaxial) domain can induce the formation of a surface step provided by the lateral growth of the normally oriented domain [shown in Fig. 3(a)]. It leads to the appearance of a basal dislocation with $\mathbf{b}=\frac{1}{3}\langle 1\,1\,\bar{2}\,0\rangle$ associated with the formation of the predicted (0 0 0 1) stacking fault.

The $\mathbf{b}=\frac{1}{3}\langle 1\,1\,\bar{2}\,0\rangle$ dislocations lying on the (0 0 0 1) basal planes near the film/substrate interface have a relative low density of $\sim 10^8\,cm^{-2}$. However, they play an important role in the elimination of TDs in the *2H* epilayer [14]. The later is schematically shown Fig. 3 and illustrated by the TEM micrographs. Our annihilation model assumes that

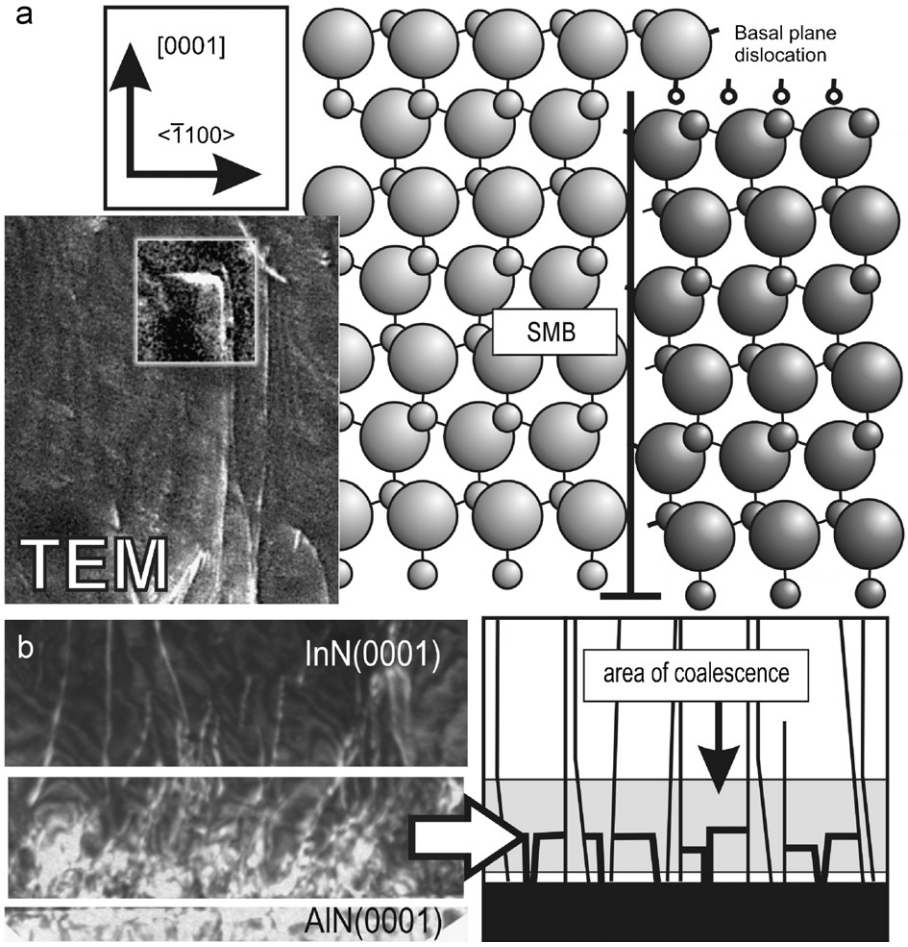

Fig. 3. Atomic plane arrangement at SMB region: (a) schematic representation of the formation mechanisms of a low-angle SMB and a basal plane dislocation as a result of coalescence process (inset: TEM image of the basal dislocation). (b) DF TEM micrographs of InN/AlN (0 0 0 1) heterostructures demonstrates a highly faulted region near the heterointerface. It is proposed that the TD density is drastically reduced due to the interaction with basal plane dislocations formed during the domain coalescence.

the interaction of $\mathbf{b} = \frac{1}{3}\langle 1\,1\,\bar{2}\,0\rangle$ TDs, generated by lattice mismatch, and basal plane stacking faults at the vicinity of domain edges along $\{0\,0\,0\,1\}$ planes leads to the bend of the TD increasing the possibility of the interaction and annihilation with other TDs. Thus, the possible termination of TDs induced by the coalescence of the misoriented (twisted and tilted) 2H domains [14,31] could be then explained as the stopping, bending, and annihilation of TDs.

Finally, the substrate temperature was found to impact drastically the coalescence of the epilayer, and consequently, the electrical and transport properties of InN material. For the samples grown at moderate temperatures of ~370 °C, homogeneous InN layers with smooth surfaces and continuous interfaces were obtained (Fig. 4(a)) Room temperature mobilities in excess of $\mu \sim 1500\,\mathrm{cm^2\,V^{-1}\,s^{-1}}$ were obtained for ~800 nm thick InN layers with the dislocation density of $\sim 3\times 10^9\,\mathrm{cm^{-2}}$ and free carrier density $n \sim 8\times 10^{17}\,\mathrm{cm^{-3}}$. Higher temperatures (~500 °C) imply the formation of initially non-coalesced InN domains with oblique shapes (Fig. 4(b)). The voids and porosities generated evolve a poor link with the pseudo-substrate, although the reduction of the active heterointerface provides an extra strain relief and a filter for the TDs arising from the substrate and reaching the growth surface. The typical electron densities and mobilities in such films show poor transport properties with $n > 5\times 10^{18}\,\mathrm{cm^{-3}}$ and $\mu < 500\,\mathrm{cm^2\,V^{-1}\,s^{-1}}$ for $a \sim 700$ nm thick InN epilayers.

4. Conclusions

In conclusion, we have examined the coalescence phenomena in thin 2H-InN epilayers. Coalescence time and the corresponding diffusion coefficients at elevated temperatures were estimated for 2H-InN overgrowth. The substrate temperature was found to impact drastically the coalescence of the epilayer, and consequently, the electrical and transport properties of InN material. Additionally, we suggest a simple growth model to explain the formation of

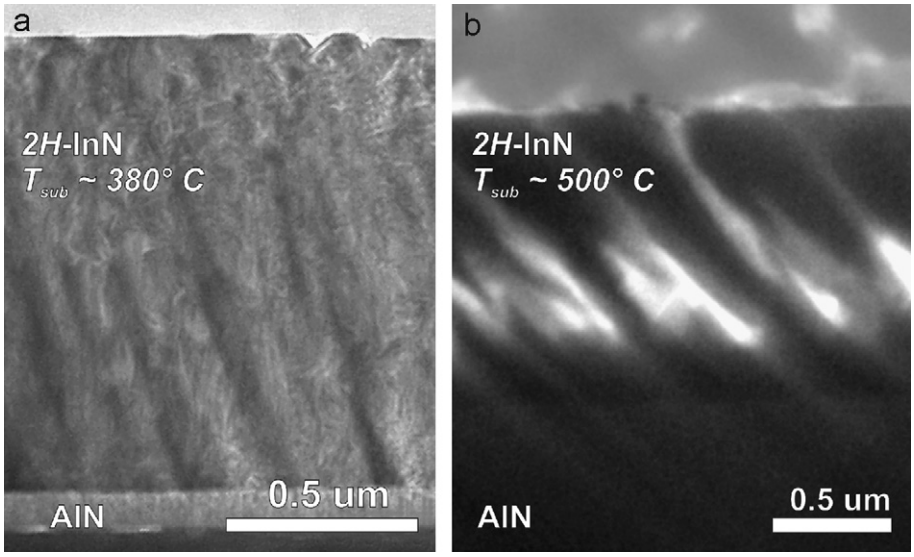

Fig. 4. (a) BF TEM micrograph of a 2.2 μm 2H-InN layer grown at ~380 °C (general view). (b) DF TEM micrograph of a 0.7 μm 2H-InN layer grown at ~500 °C.

the domain boundaries and (0 0 0 1) stacking faults formed during the coalescence. In particular, it was shown experimentally that tilted, hexagonal-shaped 2H domains form a non-coherent boundary predominantly along the $\langle 1\bar{1}00\rangle$ plane. Moreover, the local displacement of the (0 0 0 1) planes was found to be variable but not exceeding $c/2$. We also suggest that the interaction of tilted domains induces a basal dislocation to appear and annihilate due to the formation of a (0 0 0 1) stacking fault. It was demonstrated that this interaction has two obvious consequences: a lateral growth of the most normally oriented domain followed by the formation of a surface step, and consequently the termination of TDs induced by the coalescence.

Acknowledgements

This work was supported by the DFG Grant AM105/1-1 (Germany), CICYT project MAT2004-01234 (Spain), and SANDIE European Network of Excellence (NMP4-CT-2004-500101—Sixth Framework Program). F.M.M. would like to thank the Alexander von Humboldt Foundation for the financial support under a Humboldt Research Fellowship SPA/1114640STP.

References

[1] V.M. Polyakov, F. Schwierz, Appl. Phys. Lett. 88 (2006) 032101.
[2] H. Lu, W.J. Schaff, L.F. Eastman, C.E. Stutz, Appl. Phys. Lett. 82 (2003) 1736.
[3] H. Lu, W. Schaff, L. Eastman, J. Appl. Phys. 96 (2004) 3577.
[4] B. Pradarutti, G. Matthäus, C. Brückner, S. Riehemann, G. Notni, S. Nolte, V. Cimalla, V. Lebedev, O. Ambacher, A. Tünnermann, Proc. SPIE 6194 (2006) 61940I.
[5] A.G. Bhuiyan, A. Hashimoto, A. Yamamoto, J. Appl. Phys. 94 (2003) 2779.
[6] Y.F. Ng, Y.G. Cao, M.H. Xie, X.L. Wang, S.Y. Tong, Appl. Phys. Lett. 81 (2002) 3960.
[7] V. Cimalla, Ch. Förster, G. Kittler, I. Cimalla, R. Kosiba, G. Ecke, O. Ambacher, R. Goldhahn, S. Shokhovets, A. Georgakilas, H. Lu, W. Schaff, Phys. Stat. Sol. (c) 0 (2003) 2818.
[8] Y.G. Cao, M.H. Xie, Y. Liu, Y.F. Ng, H.S. Wu, S.Y. Tong, Appl. Phys. Lett. 83 (2003) 5157.
[9] S. Srinivasan, L. Geng, R. Liu, F.A. Ponce, Y. Narukawa, S. Tanaka, Appl. Phys. Lett. 83 (2003) 5187.
[10] E. Bellet-Amalric, C. Adelmann, E. Sarigiannidou, J.L. Rouvière, G. Feuillet, E. Monroy, B. Daudin, J. Appl. Phys. 95 (2004) 1127.
[11] W. Qian, M. Skowronski, M. De Graaf, K. Doverspike, L.B. Rowland, D.K. Gaskill, Appl. Phys. Lett. 66 (1995) 1252.
[12] Y. Xin, P.D. Brown, C.J. Humphreys, Appl. Phys. Lett. 70 (1997) 1308.
[13] T. Zywietz, J. Neugebauer, M. Scheffler, Appl. Phys. Lett. 73 (1998) 487.
[14] V. Lebedev, F.M. Morales, V. Cimalla, J.G. Lozano, D. González, M. Himmerlich, S. Krischok, J.A. Schaefer, O. Ambacher, Superlattices Microstruct (2006), doi:10.1016/j.spmi.2006.07.006.
[15] A.J. Bray, Adv. Phys. 43 (1994) 357.
[16] D. Weaire, S. McMurry, Solid State Phys. 50 (1997) 1.
[17] A. Kazaryan, Y. Wang, S.A. Dregia, B.R. Patton, Phys. Rev. B 63 (2001) 184102.
[18] C. Adelmann, J. Brault, G. Mula, B. Daudin, L. Lymperakis, J. Neugebauer, Phys. Rev. B 67 (2003) 165419.
[19] V. Lebedev, F.M. Morales, H. Romanus, S. Krischok, G. Ecke, V. Cimalla, M. Himmerlich, T. Stauden, D. Cengher, O. Ambacher, J. Appl. Phys. 98 (2005) 093508.
[20] L. Mandreoli, J. Neugebauer, R. Kunert, E. Schöll, Phys. Rev. B 68 (2003) 155429.
[21] G. Palasantzas, T. Vystavel, S.A. Koch, J. Th. M. De Hosson, J. Appl. Phys. 99 (2006) 024307.
[22] W.W. Mullins, J. Appl. Phys. 28 (1957) 333.
[23] L. Lewis, P. Jensen, J.-L. Barrat, Phys. Rev. B 56 (1997) 2248.
[24] F. Haußer, A. Voigt, Phys. Rev. B 72 (2005) 035437.
[25] J.E. Northrup, J. Neugebauer, L.T. Romano, Phys. Rev. Lett. 77 (1996) 103.

[26] V. Lebedev, K. Tonisch, F. Will, V. Cimalla, D. Cengher, I. Cimalla, Ch. Mauder, S. Hauguth O. Ambacher, F.M. Morales, J.G. Lozano, D. González, J. Appl. Phys. (2006), submitted for publication.
[27] J.E. Northrup, L.T. Romano, J. Neugebauer, Appl. Phys. Lett. 74 (1999) 2319.
[28] J.E. Northrup, J. Neugebauer, Phys. Rev. B 53 (1996) R10477.
[29] V. Lebedev, J. Jinschek, U. Kaiser, B. Schröter, W. Richter, J. Kräußlich, Appl. Phys. Lett. 76 (2000) 2029.
[30] V. Lebedev, J. Jinschek, J. Kräußlich, U. Kaiser, B. Schröter, W. Richter, J. Crystal Growth 230 (2001) 430.
[31] A. Bourret, C. Adelmann, B. Daudin, J. Rouvière, G. Feuillet, G. Mula, Phys. Rev. B 63 (2001) 245307.